J. Fluid Mech. (1977), *vol.* 82, *part* 2, *pp.* 261–272
Printed in Great Britain

Characterization of the formation of base sheet paper using spectral moments determined from time-series models

By WARREN R. DEVRIES† AND S. M. WU

Department of Mechanical Engineering,
University of Wisconsin, Madison

(Received 16 July 1976)

The fibre distribution in a sheet of paper, referred to as the formation, is largely the result of turbulence, a stochastic process. Continuous time-series models developed from discrete light-transmission profiles are used to characterize formation. The models are used to obtain explicit expressions for the spectral moments of the profiles. From the moments, estimates of two characteristic lengths of the fibre distribution can be obtained and are interpreted as the average and largest flock size. These lengths are used to develop an index for evaluating the formation of four samples of base sheet paper. The results of this characterization agree with other methods, but this technique has the advantage of providing a physical interpretation of the index.

1. Introduction

The distribution of fibres in a sheet of paper is referred to as the formation. Since the fibre distribution is a fundamental part of paper making, there is a need to characterize formation quantitatively so that it can be monitored during normal paper machine operation and so that changes in formation due to different operating conditions can be evaluated.

Instruments such as the Thwing–Albert and Quebec North Shore Mead formation testers have been used to analyse the paper's light-transmission profile. The Thwing–Albert tester measures the profile variance, but this single index is not based on physically meaningful parameters related to the fibre size distribution. The Quebec North Shore Mead instrument uses an analog harmonic analyser to obtain a graph of the wavelength spectrum of the profile, however the graph still requires qualitative interpretation.

Since formation is largely the result of headbox turbulence, the parameters that are used to characterize turbulence might be appropriate for characterizing formation. Two characteristic lengths derived by G. I. Taylor from the correlation function, or alternatively the spectral moments, of turbulence measurements have been suggested for this purpose. However, the sample correlation function and sample spectrum which are used to estimate these lengths are poor statistical estimates. As a result, the usefulness of this characterization technique has not been fully realized.

† Present address: Department of Mechanical Engineering, University of Michigan, Ann Arbor.

In this paper, an improved method for obtaining spectral estimates is used to evaluate the characteristic lengths derived by Taylor. The method for determining the spectrum involves finding an adequate time-series model in the form of a stochastic differential equation, which leads directly to an explicit expression for the spectrum and the necessary spectral moments. Using this approach, the formation of four base sheet samples of paper made under different operating conditions is analysed. The results of this quantitative analysis are used to rank the formation of the four samples, and this ranking is compared with both a qualitative and a Thwing–Albert evaluation made of the same samples.

2. Turbulence parameters and their relation to formation

The final distribution of fibres in a sheet of paper is affected by two interacting phenomena which occur in the fibre suspension, viz. flocculation and turbulence (Parker 1971). Flocculation is localized variation of the fibre concentration, which is a function of chemical and molecular forces and fibre morphology, which tend to draw individual fibres together to form flocks. Turbulence or localized velocity variations in the suspension create shear forces which disperse the flocks. Thus it is the equilibrium between flocculation and turbulence that produces the distribution of flocks which is observed in the paper.

Since paper formation is the result of turbulence, Reiner & Wahren (1970) and Norman & Wahren (1972) proposed that parameters derived by G. I. Taylor to characterize turbulence be used to evaluate formation. In these papers, the relation between formation and turbulence is discussed, characteristic lengths from Taylor's work are presented, and the discrete Fourier transform is suggested as a way to estimate the spectral density. However no experimental results are presented.

In his studies of diffusion in a turbulent field, Taylor (1935) defined two characteristic lengths: the macroscale and the microscale. These lengths were derived from the autocorrelation function of the stochastic velocity field. The autocorrelation of the velocity u can be expressed as a function $\rho_u(l)$ of position when an Eulerian co-ordinate system is used or as a function $\rho_u(t)$ of time when a Lagrangian co-ordinate system is used. The Eulerian co-ordinate system will be the one used in this development.

If an Eulerian set of co-ordinates is chosen then the two characteristic lengths l_1 and λ are defined by

$$l_1 \triangleq \int_0^\infty \rho_u(l)\,dl, \quad \frac{1}{\lambda^2} \triangleq -\frac{1}{2}\frac{d^2\rho_u(l)}{dl^2}\bigg|_{l=0}. \tag{1), (2}$$

The length l_1 is a measure of the minimum separation between points in the flow where the velocities are independent, i.e. a measure of how quickly the autocorrelation dies out. Taylor interpreted l_1 as the average size of eddies. A measure of the size of the smallest eddies in the flow which dissipate energy is provided by λ. This value can also be thought of as the point where a parabola tangential to $\rho_u(0)$ intersects the l axis. These two values are shown in figure 1.

An equivalent representation of the stochastic nature of the turbulent field can be given in the frequency domain. Using the definition

$$S_u(\omega) \triangleq \int_{-\infty}^{\infty} e^{-i\omega\tau}\gamma_u(\tau)\,d\tau$$

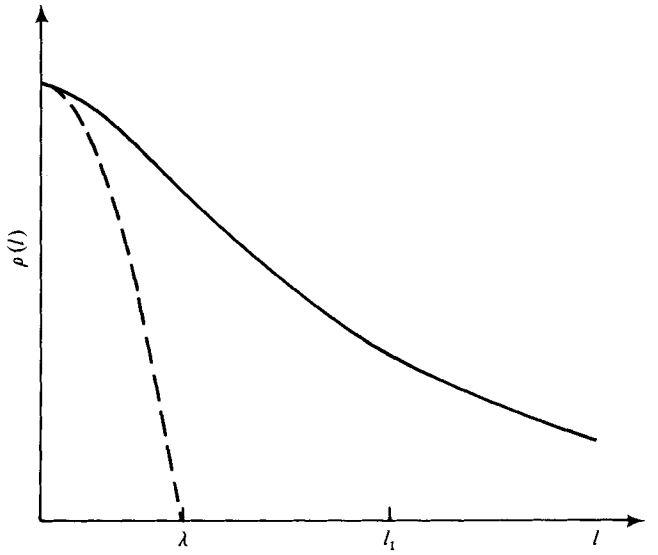

FIGURE 1. Graphical interpretation of λ and l_1 in terms of the autocorrelation function.

of the spectral density function and the properties of the moments of the spectral density gives

$$l_1 = \frac{\pi S_u(0)}{\int_{-\infty}^{\infty} S_u(\omega)\,d\omega}, \quad \frac{1}{\lambda^2} = \frac{\int_{-\infty}^{\infty} \omega^2 S_u(\omega)\,d\omega}{2(2\pi)^2 \int_{-\infty}^{\infty} S_u(\omega)\,d\omega}. \tag{3), (4}$$

Note that $\gamma_u(\tau)$ is the autocovariance function, which is related to the autocorrelation function by $\rho_u(\tau) = \gamma_u(\tau)/\gamma_u(0)$.

When measuring formation, the light-transmission profile of the paper is commonly used. The light intensity transmitted through the paper is inversely proportional to the local density variation, and hence can be used to indicate the fibre size distribution. Then, assuming that formation is isotropic, the statistical properties of the light-transmission profile can be used to characterize the formation of the base sheet paper.

Furthermore, if the light-transmission profile reflects the postulated mechanism of formation, i.e. an equilibrium between flocculation and turbulence, the macroscale and microscale for turbulence can be interpreted as parameters of the fibre size distribution in the paper. Since the final flock size is determined by shear forces which disperse the flocks, the largest flock size will be determined by the smallest eddies in the turbulent field. Thus λ can be interpreted as the largest flock size. The macroscale is defined as the average eddy size in a turbulent field, so when applied to formation l_1 can be termed an average flock size.

3. Determination of spectral moments from time-series models

The characteristic lengths l_1 and λ given by (1) and (2) in the time domain and (3) and (4) in the frequency domain are functions of the spectral moments m_0, the variance and the variance m_2 of the first derivative of the light-transmission profile. Conventional methods of estimating moments from either the sample autocorrelation

function or the sample spectrum have the disadvantages of bias and high variance. While smoothing techniques can be used to reduce the variance, a penalty is paid in terms of increased bias for a specific length of data.

Because of these problems, a different approach is used in this paper which involves first fitting a time-series model to the stochastic data. Then from the model, using the explicit expression for the spectral density, or equivalently the autocovariance function, the spectral moments are determined.

A new modelling technique termed the dynamic data system (DDS) can be used to develop a stochastic differential equation from discrete time-series data (Wu 1976). This technique involves a stepwise procedure for determining a stochastic differential equation

$$\frac{d^n X(t)}{dt^n} + \alpha_{n-1} \frac{d^{n-1}}{dt^{n-1}} X(t) + \ldots + \alpha_0 X(t) = Z(t) + b_1 \frac{dZ(t)}{dt} + \ldots + b_m \frac{d^m Z(t)}{dt_m}, \tag{5}$$

where

$$E[Z(t)\, Z(t+\tau)] = \sigma_z^2 \delta(\tau),$$

which is termed a continuous autoregressive moving-average model of order n and m, an AM(n, m) model. If the continuous stochastic process is represented by (5), then, by sampling the process $X(t)$ at uniform intervals Δ, the discrete time series $\{X_t\}$, $t = 1, 2, \ldots, N$, can be used to estimate the parameters α_i and b_i. This is done by using a difference-equation form of a model termed the uniformly sampled autoregressive moving-average (USAM) model:

$$X_t = \sum_{j=1}^{n} \phi_j(\alpha_i, \Delta)\, X_{t-j} + a_t - \sum_{j=1}^{n-1} \theta_j(\alpha_i, b_i \Delta)\, a_{t-j}, \tag{6}$$

where

$$E[a_t\, a_{t+k}] = \sigma_a^2\, \delta_k.$$

Although the form of (6) is the same as that of the familiar discrete autoregressive moving-average model, note that (6) is always of autoregressive order n and moving-average order $n-1$, and that the discrete parameters ϕ_i and θ_i are functions of the sample interval and the coefficients of the AM(n, m) model.

Once the AM model for the stochastic process $X(t)$ has been determined, the autocovariance function can be explicitly determined as

$$\gamma_X(\tau) = C_1 \exp(\mu_1 |\tau|) + C_2 \exp(\mu_2 |\tau|) + \ldots + C_n \exp(\mu_n |\tau|), \tag{7}$$

where the μ_i are the characteristic roots of (5), defined by

$$\prod_{i=1}^{n} (\mu - \mu_i) = (\mu^n + \mu^{n-1} \alpha_{n-1} + \ldots + \alpha_0) = 0,$$

and

$$C_i = -\frac{\sigma_z^2}{V \bar{V}} \sum_{j=1}^{n} \frac{R(\mu_i)\, R(\bar{\mu}_j)\, V_i \bar{V}_j}{(\mu_i + \bar{\mu}_j)},$$

with

$$V = \prod_{i=1}^{n-1} \prod_{j=i+1}^{n} (\mu_j - \bar{\mu}_i),$$

$$V_k = (-1)^{n+k} \prod_{i=1}^{n-1} \prod_{j=i+1}^{n} (\mu_j - \bar{\mu}_i), \quad i, j \neq k,$$

$$R(\mu_k) = 1 + b_1 \mu_k + \ldots + b_m \mu_k^m.$$

Here the overbars denote complex conjugates.

When the AM model is known (i.e. when the orders n and m and the parameters α_i and b_i have been estimated), the spectral density follows directly from (5) and is given by

$$S(\omega) = \frac{\sigma_z^2}{2\pi} \frac{|1 + b_1(i\omega) + \ldots + b_m(i\omega)^m|^2}{|(i\omega)^n + \alpha_{n-1}(i\omega)^{n-1} + \ldots + \alpha_0|^2}. \tag{8}$$

Estimation of the spectral density using discrete autoregressive models was proposed by Parzen (1972). However, the use of AM models is a new approach made possible by the derivation of the explicit relations between the dependent parameters of the USAM(n, m) model and the parameters of the AM(n, m) continuous model. For the case of an AM(2, 0) model, the proof of the parameter relations and the implications with regard to aliasing of the spectral estimates are discussed in Pandit & Wu (1975).

From the estimated parameters α_i and b_i of the AM(n, m) model the spectral moments

$$m_{2l} \equiv \int_{-\infty}^{\infty} \omega^{2l} S(\omega)\, d\omega$$

can be evaluated, $S(\omega)$ being given in (8). The moment integrals are of the form

$$m_{2l} = \frac{\sigma_z^2}{2\pi} \int_{-\infty}^{\infty} \frac{g_n(x)\, dx}{h_n(x)\, h_n(-x)},$$

where $x = i\omega$ and

$$\begin{aligned} g_n(i\omega) &= (i\omega)^l R(i\omega)\, (-i\omega)^l R(-i\omega) \\ &= \beta_0 + \beta_1(i\omega)^2 + \ldots + \beta_{n-1}(i\omega)^{2(n-1)}, \\ h_n(i\omega) &= (i\omega)^n + \alpha_{n-1}(i\omega)^{n-1} + \ldots + \alpha_0. \end{aligned}$$

The integral is bounded if $l + m < n$, which imposes a condition on the existence of higher-order spectral moments. The value of the moment is

$$m_{2l} = (-1)^{n-1} \sigma_z^2 M_n / 2\Delta_n, \tag{9}$$

where $\alpha_n \equiv 1$ and

$$M_n = \begin{vmatrix} \beta_{n-1} & \beta_{n-2} & \beta_{n-3} & \ldots & \beta_0 \\ \alpha_n & \alpha_{n-2} & \alpha_{n-4} & \ldots & 0 \\ 0 & \alpha_{n-1} & \alpha_{n-3} & \ldots & 0 \\ \cdot & & & & \\ \cdot & & & & \\ \cdot & & & & \\ 0 & 0 & 0 & \ldots & \alpha_0 \end{vmatrix},$$

$$\Delta_n = \begin{vmatrix} \alpha_{n-1} & \alpha_{n-3} & \alpha_{n-5} & \ldots & 0 \\ \alpha_n & \alpha_{n-2} & \alpha_{n-4} & \ldots & 0 \\ 0 & \alpha_{n-1} & \alpha_{n-3} & \ldots & 0 \\ \cdot & & & & \\ \cdot & & & & \\ \cdot & & & & \\ 0 & 0 & 0 & \ldots & \alpha_0 \end{vmatrix}.$$

The expression in (9) occurs frequently in spectral analysis and can be evaluated recursively; see for example Åström (1970).

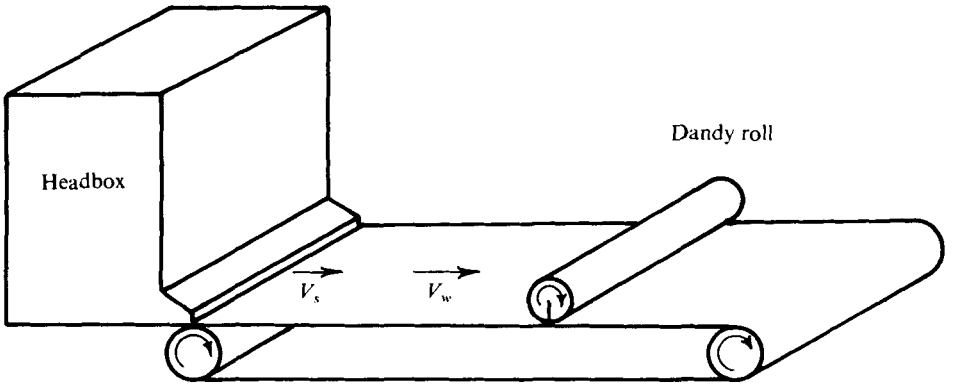

FIGURE 2. Schematic diagram of the wet end of a Fourdrinier paper machine.

Condition	Headbox consistency (%)	Drag† (ft/min)	Dandy-roll position
1	0·60	25–30	Down
2	0·75	60–70	Down
3	0·75	60–70	Up
4	0·50	0	Up

† The drag is defined as the difference between the wire velocity V_w and velocity V_s of the stock out of the headbox.

TABLE 1. Four formation conditions.

4. Characterization of formation using the characteristic lengths from AM(n, m) models

Experiments were conducted on a production paper machine (figure 2) to produce four sets of base sheet paper. During the experiments three operating variables that affect formation were varied: the headbox consistency, the drag and the dandy roll position. The settings for the operating variables for the four conditions are given in table 1. Condition 1 is the normal operating condition for this machine.

Light-transmission profiles were obtained for each of the four conditions. A laser light source and two detectors were used. A beam splitter was used to provide a reference and a transmission light beam. The ratio of the intensity of the transmitted beam to that of the reference beam served as an analog measure of the formation. A sample interval of 0·020 in. (0·51 mm) was used to digitize the analog signal and 1024 samples were taken. Condition 1, which is representative of the digitized profiles obtained in this manner, is shown in figure 3 (plate 1).

The digitized data were modelled using the DDS modelling technique and the estimation procedure outlined in the appendix. These results are summarized in table 2, which gives the order of the model, parameter estimates, and the moments m_0 and m_2 needed to determine the characteristics lengths l_1 and λ. Note that the form of the models presented in table 2 is different from the general form given by (5). The coefficient $\alpha_0 \equiv 1$ while a coefficient α_n is introduced. This parameterization is obtained

Condition	Model	$\alpha_3 \times 10^{-6}$	$\alpha_2 \times 10^{-4}$	$\alpha_1 \times 10^{-2}$	$b_1 \times 10^{-3}$	$\sigma_z^2 \times 10^{-3}$	$m_0 \times 10^{-3}$	$m_2 \times 10$
1	AM (2, 0)		5·2930	3·9692		1·3327	16·79	3·172
2	AM (3, 0)	2·5325	5·8237	6·2702		3·8686	33·15	5·692
3	AM (3, 1)	2·9396	8·2644	6·3429	−6·8027	4·2281	37·29	8·540
4	AM (2, 0)		4·5314	4·3416		1·9763	22·76	5·023

TABLE 2. AM models and spectral moments for four formation conditions.

$$\alpha_3 \frac{d^3}{dt^3} X(t) + \alpha_2 \frac{d^2}{dt^2} X(t) + \alpha_1 \frac{d}{dt} X(t) + X(t) = Z(t) + b_1 \frac{d}{dt} Z(t).$$

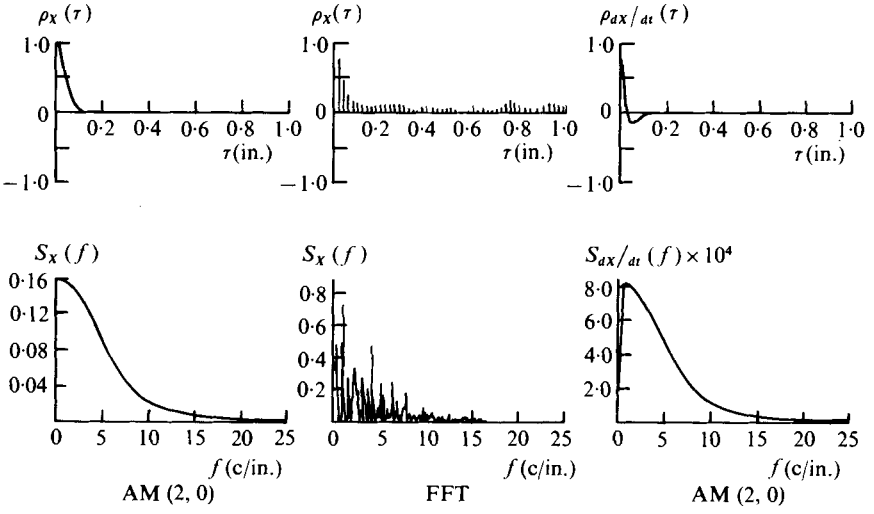

FIGURE 4. Autocorrelation and spectral density functions determined from an AM(2, 0) model and using the fast Fourier transform (FFT) for condition 1.

by dividing (5) by α_0, so that σ_z^2 is divided by α_0^2. The result of this transformation is that $Z(t)$, the white-noise process, has the same units as $X(t)$.

A representative autocorrelation function $\rho(\tau)$ and spectral density $S(\omega)$ for both $X(t)$ and the slope determined by modelling the data are shown in figure 4, with the sample autocorrelation and spectral density calculated using the fast Fourier transform provided for comparison. The plots show that by modelling the data smoothed estimates of the autocovariance and spectral density are obtained. In addition the estimates are explicit functions that can be used to evaluate the characteristic lengths associated with formation.

Using the moments from table 2 and the spectral density, the characteristic lengths for the macroscale and microscale were evaluated using (3) and (4). However, qualitative evaluation of formation by viewing a sheet of paper with transmitted light favours those sheets which have a relatively large range of fibre sizes but a small average structure. Thus a quantitative index based on the ratio of λ and l_1 will indicate better formation if the range of sizes is large relative to the average size.

To evaluate this hypothesis, λ/l_1 was calculated and compared with the results obtained with a Thwing–Albert formation tester (large values of the Thwing–Albert

Condition	λ = largest size (in.)	l_1 = average size (in.)	λ/l_1 from model	Thwing–Albert index
1	0·2044	0·0397	5·1486 (1)†	128·5 ± 10·5‡ (1)
2	0·2144	0·0584	3·6712 (3)	91·5 ± 1·5 (3)
3	0·1857	0·0567	3·2751 (4)	88·0 ± 4·0 (4)
4	0·1892	0·0434	4·3594 (2)	100·0 ± 3·0 (2)

† Numbers in parentheses indicate rank; 1 is best. ‡ Based on two tests.

TABLE 3. Characterization and ranking using AM models.

index indicate 'good' formation). The characteristic lengths λ and l_1 determined from the AM models and a comparison of the index λ/l_1 with the Thwing–Albert results are summarized in table 3. Note that the rankings obtained by the two methods agree. However the index determined from the AM models can be related to the physical characteristics of the fibre distribution.

In addition, a qualitative evaluation was made by viewing the base sheet with transmitted light. On the basis of experience, the concensus was that condition 3 was definitely the poorest formation. Condition 1 was rated better than conditions 2 and 4, but the exact rankings of conditions 2 and 4 differed among observers.

From table 3, the largest fibre sizes λ for conditions 1 and 2 are about the same (0·2044 and 0·2144 in.) while conditions 3 and 4 form a second class with λ's of 0·1857 and 0·1892 in. respectively. Considering the operating conditions listed in table 1, this grouping by λ could be attributed to the dandy roll, which was down for conditions 1 and 2 and up for conditions 3 and 4. The average fibre size given by l_1 in table 3 indicates the fibre size distributions for these four conditions. Conditions 1 and 4 give a smaller average size (0·0397 and 0·0434 in.) than conditions 2 and 3 (0·0584 and 0·0567 in.). The operating conditions suggest that low headbox consistency and drag may be responsible for the smaller average fibre size.

Another comparison can be made by using the wavelength spectral density $S(\lambda)$, which is evaluated by means of the transformation

$$\lambda = 2\pi/\omega,$$

$$S(\lambda) = S\left(\omega = \frac{2\pi}{\lambda}\right)\left|\frac{d\omega}{d\lambda}\right|.$$

In figure 5, $S(\lambda)$ is plotted for conditions 1–4 and indicates the fibre size distribution in a manner similar to the graphical results obtained with a Quebec North Shore Mead formation tester. Qualitatively, the plots for conditions 1 and 4 and for conditions 2 and 3 are similar, but it is difficult to make a quantitative assessment of the formation on the basis of the plots alone. However, on considering the λ/l_1 values in table 3, it can be seen that they can be placed in two categories which are consistent with the qualitative classification of the plots.

Finally, when using the AM models to obtain spectral moments for evaluating λ and l_1, it is assumed that the light-transmission profile is steady. If the profile is unsteady, owing to instrumentation drift, for example, the results determined with this method (and others) can be misleading. Under these circumstances, the source of the unsteadiness should be investigated or compensated for by using a deterministic component in (5).

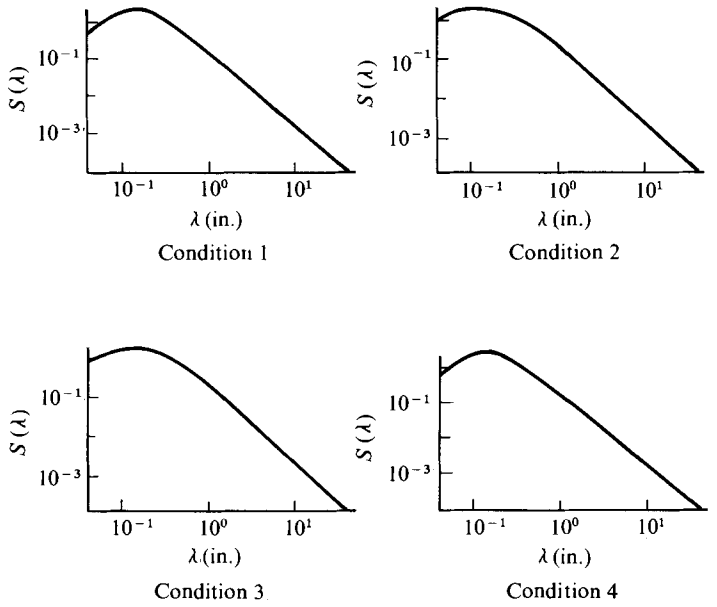

FIGURE 5. Wavelength spectral density functions determined from AM models.

5. Conclusions

A technique for characterizing and quantitatively ranking formation, the flock size distribution in a sheet of paper, was used to evaluate base sheet samples made under four paper machine operating conditions. This approach uses physically meaningful parameters related to the fibre size distribution. These parameters can be estimated by developing a time-series model for a discrete light-transmission profile in the form of a stochastic differential equation. Specific conclusions are the following.

(i) Two characteristic lengths, λ, a measure of the largest flock size, and l_1, a measure of the average flock size, can be used to characterize formation. Both are defined in terms of the spectral moments m_0 and m_2 of a light-transmission profile of a paper sample. Moreover, these lengths can be interpreted in terms of turbulence, a mechanism generating the flock size distribution.

(ii) Explicit expressions for the spectral density and spectral moments can be obtained using AM time-series models determined from discrete light-transmission profiles. Although the models may differ for different operating conditions, the spectral densities are similar.

(iii) A single index l_1/λ was used to rank the formations of four paper samples made under different conditions. This ranking agreed with a Thwing–Albert tester and qualitative evaluation, however the physical interpretation and quantitative results make the ratio l_1/λ more appealing.

(iv) On the basis of the process variables considered and the interpretation of λ and l_1, it appears that the dandy roll reduces the largest flock size λ, while low headbox consistency and low drag reduce the average flock size.

The authors wish to express their thanks to Consolidated Papers, Inc., Wisconsin Rapids, Wisconsin, for their financial support of this research. Their work in developing the laser instrument used to obtain the data for this paper was sincerely appreciated.

Appendix. Estimation of AM time-series model parameters from discrete data

Estimation of the parameters α_i and b_i in the AM(n, m) model

$$\frac{d^n}{dt^n}X(t)+\alpha_{n-1}\frac{d^{n-1}X(t)}{dt^{n-1}}+\ldots+\alpha_0 X(t) = Z(t)+b_1\frac{dZ(t)}{dt}+\ldots+b_m\frac{d^mZ(t)}{dt^m} \qquad \text{(A 1)}$$

from N discrete data X_t sampled at uniform intervals Δ is a nonlinear estimation problem. The function to be minimized is

$$\sum_{t=1}^{N} a_t^2$$

from the discrete USAM(n, m) model

$$X_t = \sum_{j=1}^{n}\phi_j(\alpha_i, \Delta)\, X_{t-j}+a_t-\sum_{j=1}^{n-1}\theta_j(\alpha_i, b_i, \Delta)\, a_{t-j}. \qquad \text{(A 2)}$$

The estimation procedure involves selecting parameters α_i and b_i, evaluating ϕ_j and θ_j from these parameters and using (A 2) to compute the sum of the squares of the a_t. Computer programs using nonlinear techniques such as Gaussian, gradient or Marquart compromise algorithms have been used to minimize the sum of the squares of a_t.

For given n and m, the fundamental parameter relations used to determine the ϕ_j and θ_j from the parameters α_i and b_i are as follows.

(i) The roots μ_i of the characteristic equation

$$\mu^n+\alpha_{n-1}\mu^{n-1}+\ldots+\alpha_0 = \prod_{i=1}^{n}(\mu-\mu_i). \qquad \text{(A 3)}$$

(ii) From the roots μ_i the coefficients ϕ_j are calculated subject to

$$(\lambda^n-\phi_1\lambda^{n-1}-\ldots-\phi_n) = \prod_{i=1}^{n}(\lambda-\lambda_i), \qquad \text{(A 4)}$$

where $\lambda_i = \exp(\mu_i\Delta)$.

(iii) The coefficients θ_j are evaluated from the relation

$$\theta_j = \frac{\sum_{i=1}^{n}\sum_{k=1}^{n} R(\mu_i)\overline{R(\mu_k)}\, V_i\overline{V}_k\left(\frac{\lambda_i\overline{\lambda}_k-1}{\mu_i+\overline{\mu}_k}\right)\sum_{l=0}^{j}\phi_l\lambda_i^{(j-l)}}{\sum_{i=1}^{n}\sum_{k=1}^{n} R(\mu_i)\overline{R(\mu_k)}\, V_i\overline{V}_k\left(\frac{\lambda_i\overline{\lambda}_k-1}{\mu_i+\overline{\mu}_i}\right)}, \qquad \text{(A 5)}$$

where

$$\phi_0 = -1, \quad R(\mu_i) = 1+\sum_{j=1}^{m} b_j\mu_i^j,$$

$$V_k = (-1)^{n+k}\prod_{i=1}^{n-1}\prod_{j=i+1}^{n}(\mu_j-\overline{\mu}_i), \quad i,j \neq k.$$

An AM(n, m) model is adequate when changing the orders n and m of the model causes no significant reduction in the sum of the squares of the a_t and the a_t are un-

correlated. The test for no significant improvement is based on an F-test. If n and m are increased simultaneously, usually in steps of two, and

$$\frac{(\Sigma a_t^{2(0)} - \Sigma a_t^{2(1)})/(\delta n + \delta m)}{\Sigma a_t^{2(1)}/(N - n - \delta n - m - \delta m)} < F_\alpha(\delta n + \delta m, N - n - \delta n - m - \delta m), \tag{A 6}$$

where

$$\Sigma a_t^{2(0)} = \text{sum of squares for AM}(n, m),$$

$$\Sigma a_t^{2(1)} = \text{sum of squares for AM}(n + \delta n, m + \delta m),$$

then the AM(n, m) model is adequate. Once the criterion (A 6) has been met, it is possible to simplify the model after examining the confidence intervals for the parameters and then re-estimating the model without those parameters whose confidence intervals include zero.

By the strategy outlined above, an AM model can be determined from discrete data. However, large differences in the magnitudes of the parameters α_i and b_i can cause numerical ill-conditioning during estimation. This condition is due to the nature of the data reflected by the characteristic roots μ_i. As indicated by (A 3), α_0 is the product of all the roots, α_1 is the sum of the products of $n-1$ roots, ..., and α_{n-1} is the sum of all the μ_i. If, for example, the magnitudes of the characteristic roots are of the order of 10 and an AM$(3, 0)$ model is to be estimated, then α_2, α_1 and α_0 will be of the order of 10, 100 and 1000 respectively. A similar situation occurs when the roots are less than one in magnitude.

To numerically condition the estimation problem, an approach similar to time scaling for analog computers can be used. A fictitious sample interval $\Delta^* = \Delta/a$ can be used to estimate an AM model of the same form as (A 1) but with scaled parameters α_i^* and b_i^*. From experience, the scale factor a can be selected using the initial values $\alpha_i^{(0)}$ and $b_i^{(0)}$ determined using the original sample interval Δ and the relation

$$a = \text{integer}\,[\log_{10}(\alpha_0^{(0)})/-n]. \tag{A 7}$$

When converting from α_i^* and b_i^* to α_i and b_i the transformations are

$$\left.\begin{aligned} \alpha_i &= \alpha_i^* a^{n-i}, \quad i = 0, 1, \ldots, n-1, \\ b_i &= b_i^* a^{-i}, \quad i = 1, 2, \ldots, m, \\ \mu_i &= \mu_i^* a. \end{aligned}\right\} \tag{A 8}$$

However, the parameters of the USAM model (A 2) are unchanged by this transformation.

This technique is effective in conditioning most AM(n, m) estimation problems. Furthermore, from (A 7), if a is a power of ten, then the inverse transformation given by (A 8) corresponds merely to shifting the decimal point in the parameters α_i^*, b_i^* and μ_i^*.

REFERENCES

Åström, K. J. 1970 *Introduction to Stochastic Control Theory*. Academic Press.

Norman, B. & Wahren, D. 1972 A comprehensive method for the description of mass distribution in sheets and flocculation and turbulence in suspensions. *Svensk Papperstidning* **75**, 807–818.

Pandit, S. M. & Wu, S. M. 1975 Unique estimates of the parameters of a continuous stationary stochastic process. *Biometrika* **62**, 496–503.

PARKER, J. D. 1971 Development of smaller scale structures in headbox design. *Australian Pulp Paper Indust. Tech. Ass.* **25**, 185–193.

PARZEN, E. 1972 Some recent advances in time series analysis. In *Statistical Models and Turbulence*, pp. 470–492. Springer.

REINER, L. & WAHREN, D. 1970 The characterization of flow from the headbox of a paper machine. *Svensk Papperstidning* **74**, 225–232.

TAYLOR, G. I. 1935 Statistical theory of turbulence. *Proc. Roy. Soc.* A **51**, 421–479.

WU, S. M. 1976 Dynamic data system, a new modeling approach. *A.S.M.E. Paper* 76-WA/Prod-24.

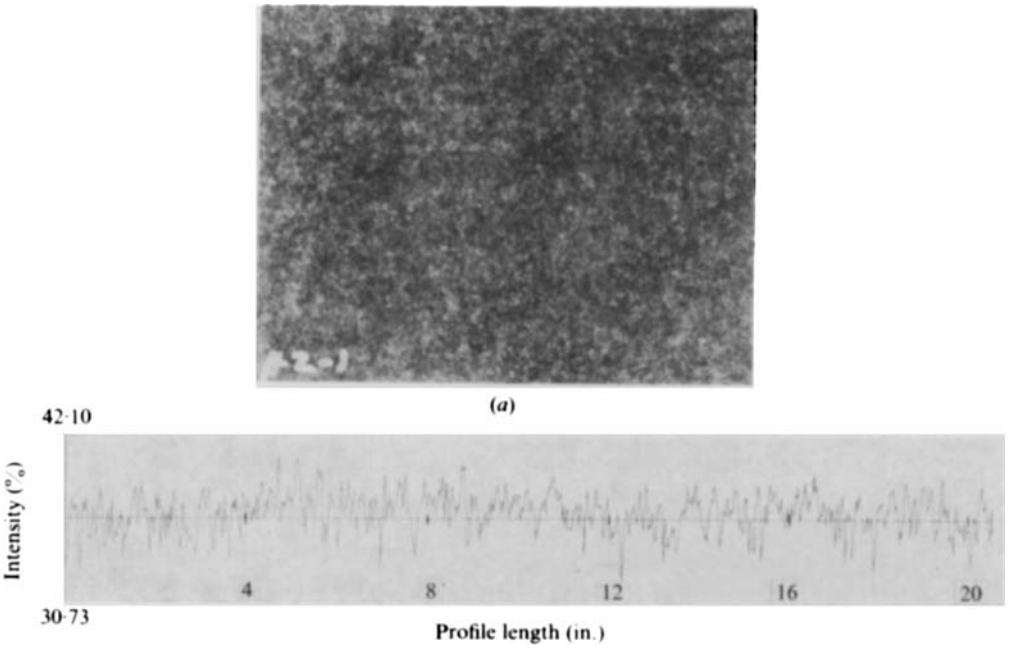

FIGURE 3. (*a*) Photograph of a 3·5 × 4·5 in. sample of base sheet paper taken with transmitted light and (*b*) digitized light-transmission profile with $\Delta = 0{\cdot}02$ in. and 1024 points for formation condition 1.